

Chapter 8

Objective Evaluation of Radiographic Contrast-Enhancement Masks

The development and application of radiographic contrast-enhancement masks (RCMs) in digital radiography (DR) were discussed in the previous chapters. The prime purpose of anatomically shaped RCMs is to reduce the dynamic range of values within a DR image. By achieving this goal, the anatomy within the image can be visualised with higher radiographic contrast.

Several other methods of achieving dynamic range control were also discussed in the previous chapter. These methods are typically unsharp mask filters with large kernel sizes, and multi-scale approaches such as multi scale image contrast amplification (MUSICA) developed by the Agfa-Gevaert company (Vuylsteke & Schoeters, 1999). In achieving their goal of dynamic range control, these methods alter the relative contributions of spatial frequencies within the image and hence the visual appearance of the image. A full discussion of these and other image processing techniques was presented in Chapter 5.

It is generally accepted that both unsharp mask filters and multi-scale approaches introduce noise into the image (Jabri & Wilson, 2002; Prokop *et al*, 1993; Vuylsteke & Schoeters, 1999). Noise degrades image quality. Noise can be introduced into images in a variety of ways, such as the image capture itself, from electronic components of the imaging system and from operations performed on the image (Castleman, 1996; Gonzalez & Woods, 1992; Jain, 1989).

Measurements of signal to noise ratio (SNR) in DR images of hand and foot phantoms were performed. The original images were modified by unsharp mask, multi-scale approaches and RCM methods. Further measurements of SNR in these modified images were made and compared with the original images. The details and results of the SNR measurements are discussed in this chapter.

8.1 Acquisition of Digital Radiographic Images

Computed radiographic images of a hand phantom and a foot phantom were obtained (3M Company, St. Paul, USA). The x-ray unit used to expose the phantoms and computed radiography (CR) image plate was a Shimadzu UD150L-30E (Shimadzu Medical Systems, Mt Waverley). Three images, posterior-anterior (PA) projection of the hand phantom, anterior-posterior (AP) projection of the foot phantom and an oblique (Obl) projection of the foot phantom, were obtained. Radiographic exposure details used in the acquisition of the images are listed in Table 8.1. The images were acquired on an ADC Solo (Agfa-Gevaert, Nunawading) CR unit and viewed through the IPD Viewer Software (Agfa-Gevaert, Nunawading).

Table 8.1 Radiographic exposure factors of the hand and foot phantoms

Phantom and Position	kVp	mAs	Focal Film Distance (cm)	Focal Spot Size (mm)
Hand – PA	55	10	100	0.6
Foot – AP	60	10	100	0.6
Foot – Obl	60	15	100	0.6

The IPD Viewer Software has MUSICA values that are routinely set depending upon the anatomical region and radiographic position preselected by the radiographer. For each of the image positions detailed in Table 8.1 the MUSICA values of MUSI contrast, latitude reduction, edge contrast and noise reduction were initially set to zero. These images were saved as “original” files and transferred to a personal computer. The extended window left, extended window right and sensitometry curve MUSICA values have an affect on the image when it is viewed on that computer using the IPD Viewer Software and do not affect the stored image.

8.2 Modification of Digital Radiographic Images

The MUSICA values of MUSI contrast and latitude reduction have the effect of dynamic range control of CR images when viewed using the IPD viewer software (IPD Viewer Software Reference Manual, 2002; Vuylsteke & Schoeters, 1999). MUSI contrast and latitude reduction are user selectable on an integer scale of 0 to 6. MUSI contrast is achieved using multi-scale approaches whereas latitude reduction uses unsharp mask filtering (IPD Viewer Software Reference Manual, 2002).

MUSI contrast and latitude reduction values were applied to each of the three images listed in Table 8.1. Each of the three images was modified using the IPD Viewer Software at each of the MUSI and latitude reduction values listed in Table 8.2. These images were then saved on to a personal computer for further analysis.

Table 8.2 MUSICA factors used for processing images listed in Table 8.1

Name	Latitude Reduction Value	MUSI Value
Original	0.0	0.0
MUSI 2	0.0	2.0
MUSI 4	0.0	4.0
MUSI 6	0.0	6.0
Lat Red 2	2.0	0.0
Lat Red 4	4.0	0.0
Lat Red 6	6.0	0.0
LR=3 M=3	3.0	3.0
LR=6 M=6	6.0	6.0

Figure 8.1 shows examples of the three images from the hand and foot phantoms. A CR image of a PA projection of the hand phantom is shown in Figure 8.1a. It is the original image without any MUSI or latitude reduction factors. Figure 8.2b is an AP projection of the foot phantom with MUSICA factors of MUSI = 6 and latitude reduction = 0. The third image, Figure 8.1c, is an example of an oblique projection of the foot phantom. MUSICA factors of MUSI = 6 and latitude reduction = 6 were used to modify this image. Edge enhancement is apparent in Figures 8.1b & c.



Figure 8.1 Computed radiographic images of phantoms with various MUSICA factors

a. Hand, PA, MUSI contrast = 0, latitude reduction = 0;

b. Foot, AP, MUSI contrast = 6, latitude reduction = 0;

c. Foot, Obl, MUSI contrast = 6, latitude reduction = 6.

8.3 Visual Comparison of Noise in the Digital Radiographic Images

Assessment of noise in images can be made subjectively or objectively. A subjective means of visualising the effects of noise in an image is by viewing a one-dimensional (1D) plot or transect across the image. This technique provides a plot of pixel values versus distance across the image (Badano, Gagne & Jennings, 2004; Baxes, 1994; Celenk, 1990).

The PA projection of the hand phantom was arbitrarily chosen as the image on which to undertake the visualisation of image noise. Each image modified with various MUSICA factors, and a RCM modified image was included in the comparison. One-dimensional (1D) transects of these images were compared to the original image. For uniformity of comparison, the spatial locations of the 1D transects were the same in all images. Figure 8.2 shows the spatial location of the 1D transects as a line on the image.

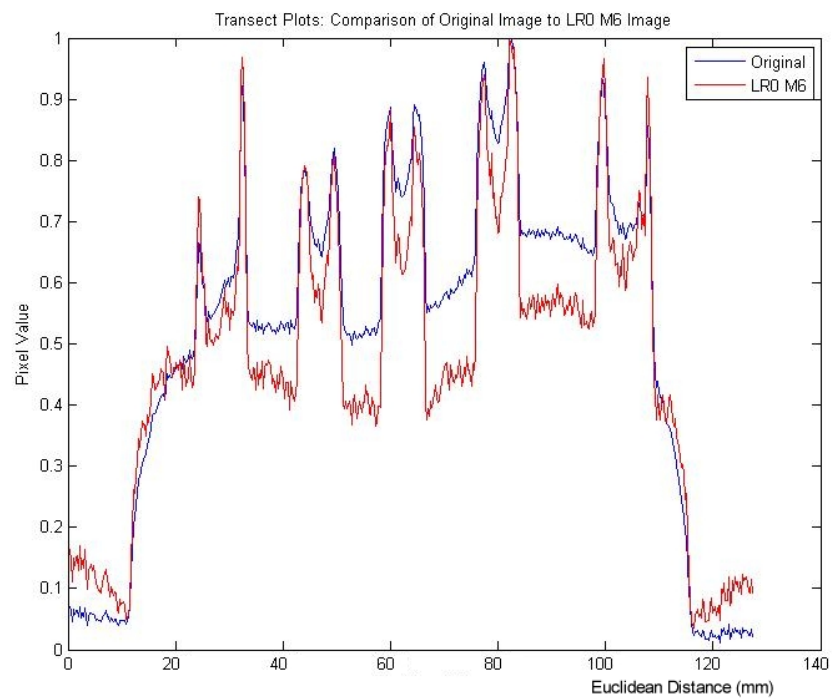
1D transects of images of the hand phantom were created using Matlab[®] (MathWorks Inc., Natick, USA) mathematical software. These transects are shown in Figures 8.3a–d. In all of these plots, the blue line represents the original image and the red line represents the modified image. In each plot, the pixel value has been normalised for comparison between transects of the images. The X-axis of each plot is the Euclidean distance across the image. A wedge RCM was used to modify the original image. The wedge RCM factors are listed in Table 8.3.



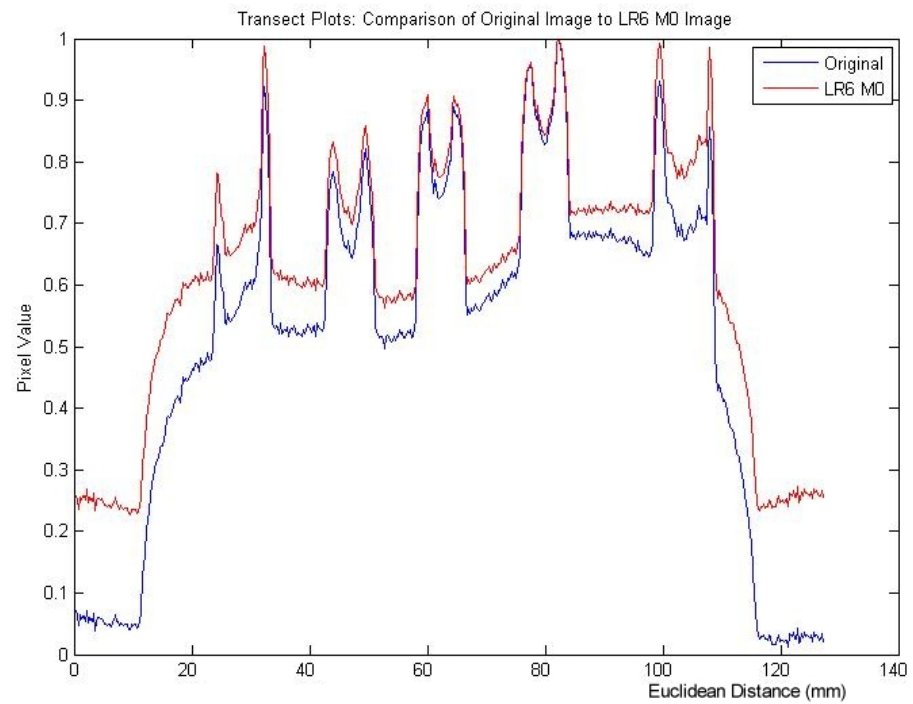
Figure 8.2 PA projection of the hand phantom showing the location of the 1D transects

Table 8.3 RCM factors for the PA hand image

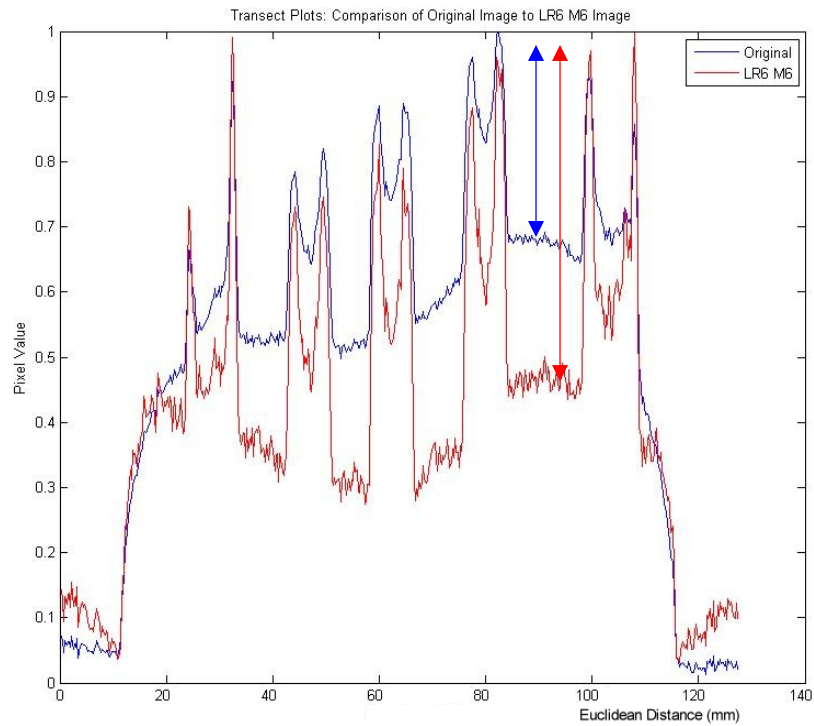
User selectable factors
curved or linear: linear
end vector lengths (%) non-enhanced: 0 enhanced: 0
rotation: 180°
profile height: 4.0



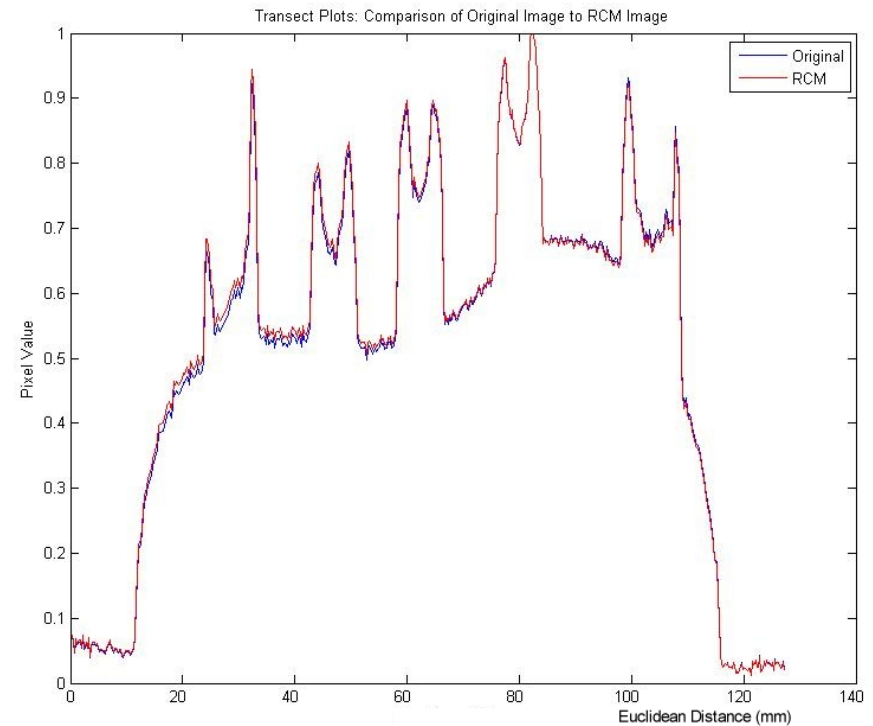
a.



b.



c.



d.

Figure 8.3 Transect plots of the hand phantoms with various MUSICA factors and of a RCM image showing normalised pixel values over the Euclidean distance (mm) of the pixels within the images

- a. Original image (blue) compared to MUSI 6 image (red) – MUSI factor = 6, latitude reduction = 0;
- b. Original image (blue) compared to Lat Red 6 image (red) – MUSI factor = 0, latitude reduction = 6;
- c. Original image (blue) compared to LR=6 M=6 image (red) – MUSI factor = 6, latitude reduction = 6; arrows indicate the difference between the bone and soft tissue pixel value, blue indicates the difference in the original image and red in the enhanced image;
- d. Original image (blue) compared to RCM image (red).

Visual comparison of the three MUSICA transects of the modified images to the original image in Figures 8.3a, b & c clearly indicates the increase in difference between pixel values at edges within the image, in this case the bone–soft tissue interface. These plots visually demonstrate the edge enhancement effect of these methods of dynamic range control. This is visualised on the plots as an increased vertical distance between the pixel values representing bone and those representing the soft tissue in the MUSICA image transect compared to the same spatial locations in the original images transect. These are indicated by the red and blue arrows in Figure 8.3c. No edge enhancement effect is visualised in Figure 8.3d, the transect comparison between the original and RCM modified images.

Also visualised in Figures 8.3a, b & c is the noise that is introduced into the images by the MUSICA methods. The noise can be visualised as increased variations of the plot in relatively uniform regions, such as the low pixel value regions between the carpal bones. In comparison, the same regions in the RCM method plot do not show the same amount of variation as to the original image.

8.4 Measurement of Signal to Noise Ratio in the Digital Radiographic Images

Measurement of image noise or SNR measurement has been undertaken by various authors to aid in the comparison of image quality (Ciantar *et al*, 2000; Haiter-Neto & Wenzel, 2005; Samei *et al*, 2005). In this project, SNR measurements were made to compare the quality of the images that were modified by MUSICA factors and by RCM methods. Images from the three phantoms were measured. The SNR measurements of the original image, that is, the images that have not undergone modification, are considered the “gold standard”. The modified images were compared to the original images.

Measurements of SNR, in decibels (dB), were made for each original image and for the eight modified images using the formula in Equation 8.1. Using this method, the SNR will equal zero where the variance of the noise is equal to variance of the

signal. Larger SNR values imply less corruption by noise in the image than lower SNR values (Calway, 1999).

$$SNR_I = 10 \cdot \log_{10} \frac{\sigma_I^2}{\sigma_n^2} \quad \dots\dots\dots 8.1$$

(adapted from Calway, 1999, p. 31)

where σ_I^2 is the variance of the image and σ_n^2 is the variance of the noise

Each of the original and modified images was visualised and SNR measurements were made using Matlab[®]. The area in the image without attenuation of x-ray radiation (i.e. adjacent to the phantom) was used to measure the variance of noise. This is a uniform area within the image, and any variations within it can be considered as a measurement of noise only. The signal was measured in regions of interest (ROI) within the image of the phantom. In each image, five different SNR measurements were made at different signal and noise ROIs. Examples of where signal and noise measurements were made are shown in Figures 8.4a, b & c.

Results of SNR measurements are shown in Tables 8.3a, b & c. Each table lists the image details and the average SNR value from the five measurements. The ratio of the image SNR value to the original image SNR value is given. The standard deviation of the SNR measurements is also provided.

Graphical displays of these results are shown in Figures 8.5a, b & c. Figure 8.5a shows measurements of the relative SNR of various MUSI values when the latitude reduction was not used to modify the image. Relative SNR of various latitude reduction factors when the MUSI values were not used to modify the image can be seen in Figure 8.5b. When a mix of both MUSI and latitude reduction factors were used in the images, relative SNR values were as shown in Figure 8.5c. In all graphs, the error bars represent the standard deviation of SNR measurements. The combined values of relative SNR for all three phantom images are also shown.



a.

b.

c.

Figure 8.4 Images of phantoms showing regions of interest for the measurement of noise (large rectangle) and image signal (small rectangle with cross) a. PA hand image; b. AP foot image; c. Oblique foot image

Table 8.3 Signal to noise ratio (SNR) measurements of the original, MUSICA and RCM modified images for each radiographic phantom

- a. PA image of the hand phantom;
- b. AP image of the foot phantom;
- c. Oblique image of the foot phantom.

a. **Hand PA**

Image	MUSICA Factors		SNR Values		Ratio
	LR*	M**	Ave (dB)	St Dev (dB)	
Original	0	0	10.830	3.576	1.000
MUSI 2	0	2	9.657	4.263	0.892
MUSI 4	0	4	9.026	4.184	0.833
MUSI 6	0	6	8.379	3.773	0.774
Lat Red 2	2	0	10.254	4.798	0.947
Lat Red 4	4	0	6.966	4.844	0.643
Lat Red 6	6	0	4.055	5.627	0.374
LR=3 M=3	3	3	9.808	3.200	0.906
LR=6 M=6	6	6	8.552	1.458	0.790
RCM	0	0	10.965	3.108	1.012

b. **Foot AP**

Image	MUSICA Factors		SNR Values		Ratio
	LR*	M**	Ave (dB)	St Dev (dB)	
Original	0	0	17.236	5.335	1.000
MUSI 2	0	2	16.208	5.500	0.940
MUSI 4	0	4	12.073	4.269	0.700
MUSI 6	0	6	11.289	2.562	0.655
Lat Red 2	2	0	8.101	9.274	0.470
Lat Red 4	4	0	-0.251	11.594	-0.015
Lat Red 6	6	0	-6.551	14.315	-0.380
LR=3 M=3	3	3	3.902	7.524	0.226
LR=6 M=6	6	6	5.035	3.427	0.292
RCM	0	0	17.125	6.134	0.994

c. **Foot Obl**

Image	MUSICA Factors		SNR Values		Ratio
	LR*	M**	Ave (dB)	St Dev (dB)	
Original	0	0	10.205	1.461	1.000
MUSI 2	0	2	9.589	0.934	0.940
MUSI 4	0	4	7.494	1.735	0.734
MUSI 6	0	6	7.600	2.206	0.745
Lat Red 2	2	0	-0.985	3.643	-0.096
Lat Red 4	4	0	-8.084	6.749	-0.792
Lat Red 6	6	0	-11.056	7.550	-1.083
LR=3 M=3	3	3	1.049	3.802	0.103
LR=6 M=6	6	6	3.289	3.524	0.322
RCM	0	0	9.621	1.519	0.943

* LR = latitude reduction

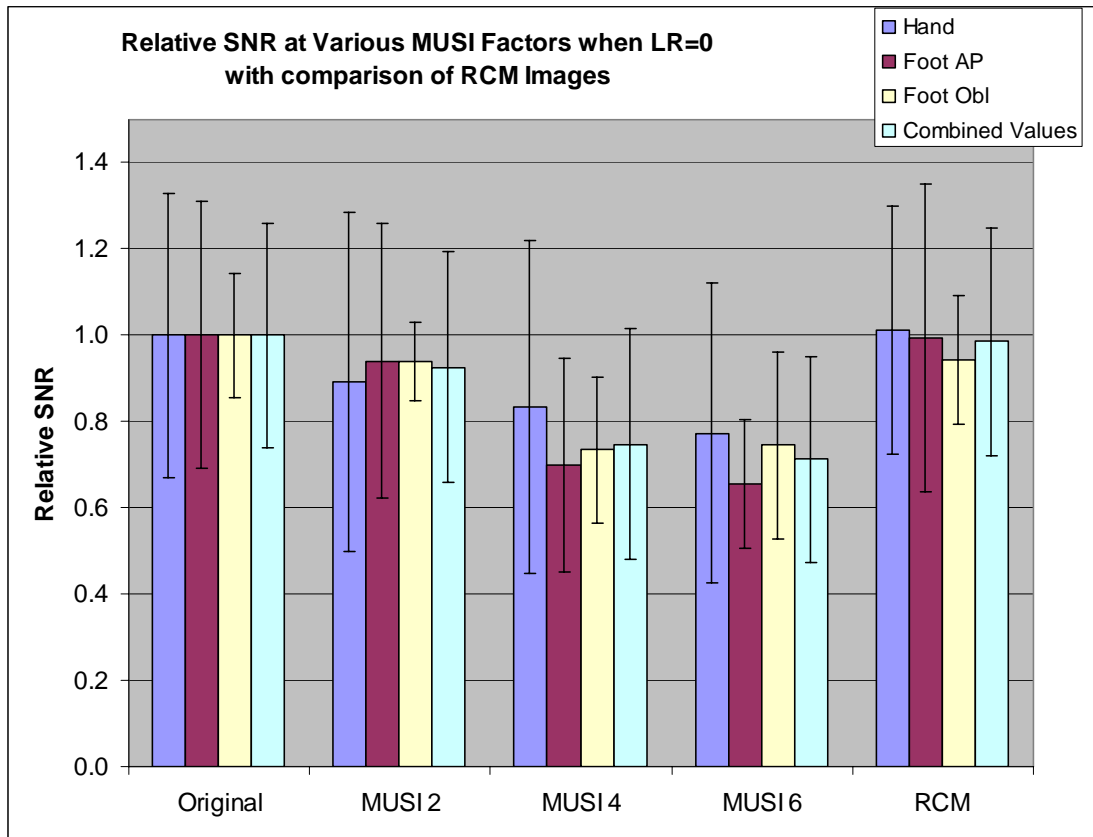
** M = MUSI factor

For all images that were modified using various levels of MUSICA factors, SNR was lower than that of the original image. These measurements are in agreement with Vuylsteke & Schoeters (1999) who showed that these methods reduce the SNR within the image.

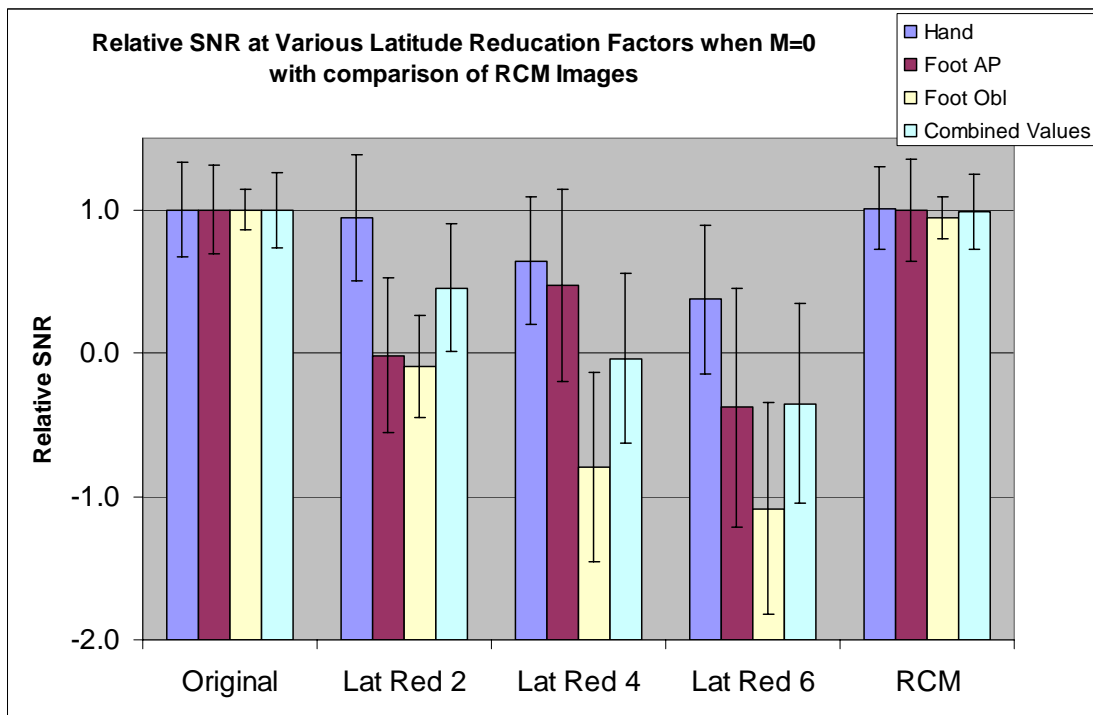
When the images were modified using only multi-scale approaches, that is, when the latitude reduction setting was zero, less noise was introduced into the image than when unsharp mask filters were used. A direct comparison of the SNR reduction between images with only MUSI factors, latitude reduction factors, and when a mixture of both was used is shown graphically in Figure 8.6. Of all approaches measured, the unsharp mask filter introduced the most noise into the images.

The images modified with RCM approaches had similar SNR to the original images. All of the RCM modified images had higher SNR than the MUSICA modified images. This suggests that the RCM approach did not introduce additional noise into the images.

a.



b.



C.

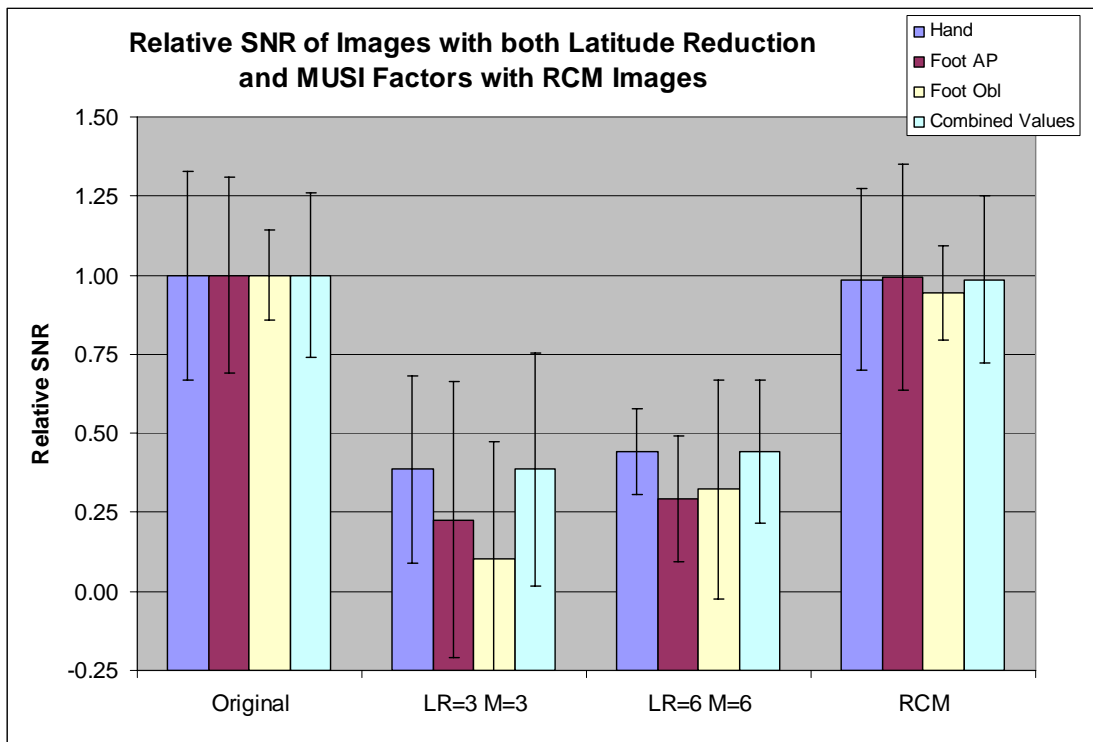


Figure 8.5 Plots of relative SNR of the PA hand, AP foot, oblique foot images and combined values.

Error bars show standard deviation of the SNR measurements

- a. Original image, images with various MUSI factors and lat red = 0 and RCM image
- b. Original image, images with various lat red factors and MUSI = 0 and RCM image
- c. Original image, images with various MUSI and lat red factors and RCM image

Note: LR = latitude reduction; M = MUSI factor; RCM = radiographic contrast-enhancement mask

8.5 Noise in Radiographic Contrast-Enhanced Digital Radiographic Images

Transect plots of RCM-enhanced images graphically (Figure 8.3d) show little change in terms of noise in the image compared to the original image. Measurements of SNR show only minor variations between the RCM-enhanced images and the original DR image.

These results were expected. The application of a RCM to a DR image does not change the spatial appearance of the image. The RCM method changes only the local

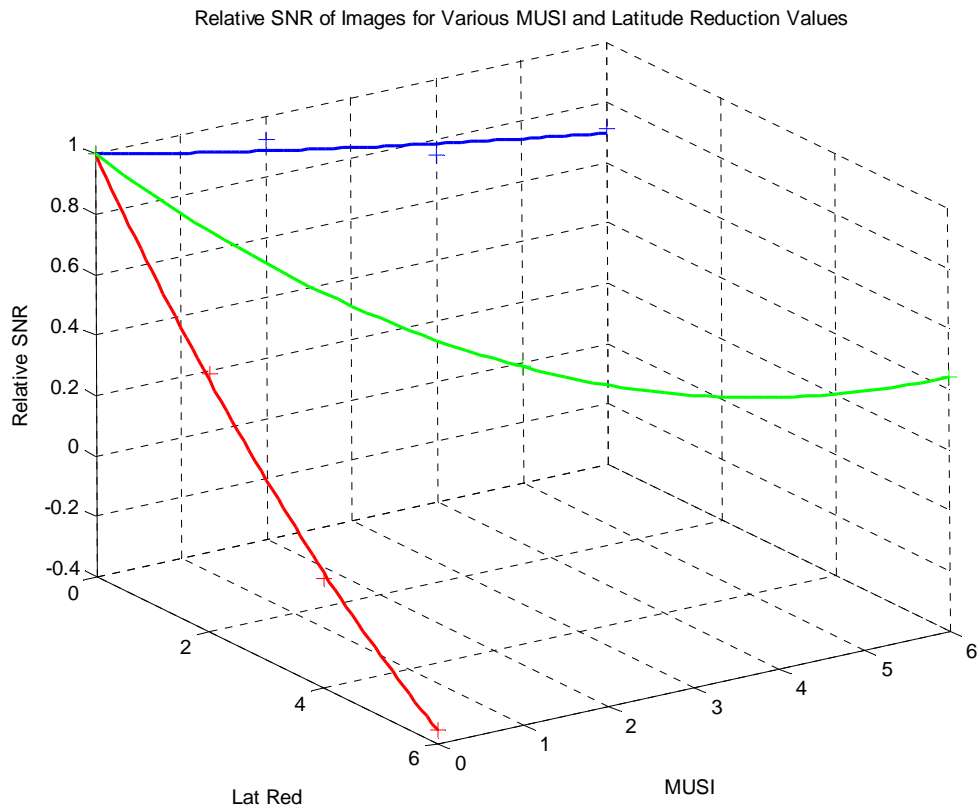


Figure 8.6 Three-dimensional graphical display of the decrease of relative SNR when various MUSI and latitude reduction factors were used to modify the images. (Combined results of image SNR of all phantoms)
 Red – MUSI factors were zero
 Blue – Latitude reduction factors were zero
 Green – Combined MUSI and latitude reduction factors
 + indicates measured values and the solid lines are polynomial lines of best fit to the measured data.

contrast in its endeavour to reduce the dynamic range of the image. Multi-scale approaches and unsharp mask filters inherently change the spatial appearance of the image in achieving their goal of dynamic range reduction.

As an objective measure of medical image quality, SNR has been the subject of debate (Ciantar *et al*, 2000; Erdonogmus *et al*, 2004). Whereas radiographic images are assessed subjectively in daily clinical radiographic practice, objective measurements of radiographic images in daily clinical practice are rarely performed. Subjective evaluation of the RCM method and resulting images was undertaken. The next two chapters detail the approaches taken and the results of subjective evaluation of the RCM modified images.